A more detailed discussion concerning the optimization procedure will be presented in a forthcoming report.

ACKNOWLEDGMENT

The authors would like to acknowledge Dr. A. Kerr at the Goddard Space Institute, NY, for kindly lending us his computer program, and T. Ståhlberg for some calculations on mixer performance. They would also like to thank C. O. Lindström for carrying through many of the experiments.

REFERENCES

[1] R. A Linke, M. V. Schneider, and A. Y. Cho, "Cryogenic millimeter-wave receiver using molecular beam epitaxy diodes," *IEEE Trans. Microwave Theory Tech.*, vol. MTT-26, pp. 935–938, 1978.
[2] N. Keen, R. Haas, and E. Perchtold, "Very low noise mixer at 115 GHz using a Mott diode cooled to 20 K," *Electron. Lett*, vol. 14, pp. 825–826.
[3] A. V. Räisänen, N. R. Erickson, J. L. R. Marrero, P. F. Goldsmith, and C. R. Predmore, "An ultra low-noise Schottky mixer receiver at 80–120 GHz," presented at the 1981 IEEE Int. Conf. on Infrared and Millimeter Waves, Miami Beach, Florida, Dec. 7–12, 1981.
[4] B. Vowinkel, J. K. Peltonen, W. Reinhert, K. Grüner, and B. Aumiller, "Airborne imaging system using a cryogenic 90-GHz receiver," *IEEE Trans. Microwave Theory Tech.*, vol. MTT-29, pp. 535–541, 1981.
[5] M. Feldman and S. Rudner, *Reviews Infrared Millimeter Waves*, vol. II, 1982.
[6] T. J. Viola and R. J. Mattauch, "Unified theory of high-frequency noise in Schottky barriers," *J Appl. Phys.* vol 44, pp. 2805–2808, 1973.
[7] R. L. Eisenhart and P. J. Kahn, "Theoretical and experimental analysis of a waveguide mounting structure," *IEEE Trans. Microwave Theory Tech.*, vol. MTT-19, pp. 706–719, 1971.
[8] C. E. Hagström and E. L. Kollberg, "Measurements of embedding impedance of millimeter-wave diode mounts," *IEEE Trans. Microwave Theory Tech.*, vol. MTT-28, pp. 899–904, 1980.
[9] M. Pospieszalski and S. Weinreb, "A method for measuring an equivalent circuit for waveguide-mounted diodes," in *Proc. 10th Eur. Microwave Conf.* (Warszawa, Poland), Sept. 1980.
[10] M. Pospieszalski and S. Weinreb, "A method for measuring an equivalent circuit for waveguide-mounted diodes," National Radio Astronomy Observatory, Charlottesville, VA, Electronics Division Internal Rep. 201, Oct. 1979.
[11] N. H. Held and A. R. Kerr, "Conversion loss and noise of microwave and millimeter-wave mixers: Parts 1 and 2," *IEEE Trans. Microwave Theory Tech.*, vol. MTT-26, pp. 55–70, Feb. 1978.
[12] N. J. Keen, "Low-noise millimeter-wave mixer diodes, results and evaluation of a test programme," *Proc IEEE*, vol. 127, pp. 188–198, Aug. 1980.
[13] H. Zirath, E. Kollberg, M. V. Schneider, A. Y. Cho, and A. Jelenski, "Characteristics of metal-semi-conductor junctions for mm-wave detectors," in *Proc. 7th Int. Cont. Infrared millimeter waves*, (Marseille, France), Feb. 1983.

Hyperabrupt Junction Varactor Diodes for Millimeter-Wavelength Harmonic Generators

KEITH LUNDIEN, MEMBER, IEEE,
ROBERT J. MATTAUCH, SENIOR MEMBER, IEEE, JOHN ARCHER,
AND ROGER MALIK, MEMBER, IEEE

***Abstract*—The design of a hyperabrupt Schottky-barrier varactor is considered with an exponentially retrograded doping profile assumed. Resistance and capacitance models are used to determine optimum doping profile characteristic length and breakdown voltage with respect to device dynamic cutoff frequency. Device fabrication is discussed and test results are presented indicating conversion efficiencies of approximately 15 percent upon doubling to the 200-GHz frequency range.**

Manuscript received June 2, 1982; revised September 9, 1982. This work was supported in part by the National Science Foundation under Grant EC580-22937, and by the National Radio Astronomy Observatory which is operated by Associated Universities, Inc., under contract with the National Science Foundation.

K. Lundien is presently with General Electric, Portsmouth, VA.
R. Mattauch is with the Department of Electrical Engineering, University of Virginia, Charlottesville, VA.
J. Archer is with the National Radio Astronomy Observatory, Charlottesville, VA.
R. Malik is with the U.S. Army Electronics Technology and Devices Laboratory, ERADCOM, Fort Monmouth, NJ 07703.

I. INTRODUCTION

Due to recent improvements in the conversion efficiency, and output power of GaAs-Schottky-barrier varactor harmonic generators, solid-state sources are replacing expensive and short-lived klystrons as local oscillators in the 100–230-GHz range. This paper extends the work of Archer *et al.* [1] in the optimization of devices for harmonic generation by taking advantage of the increased voltage sensitivity of hyperabrupt junction device capacitance.

For the same voltage variation, the capacitance of a hyperabrupt junction changes more than that of a comparable abrupt junction device. This results in a greater power conversion efficiency because the relative magnitude of each output harmonic depends upon the nonlinearity of the capacitance–voltage law. This paper is concerned with the selection of the optimal device fabrication parameters: impurity doping profile, epitaxial layer thickness, and anode size to provide the maximum cutoff frequency and output power for a given breakdown voltage.

II. DEVICE STRUCTURE

The impurity doping profile examined in this study was exponentially retrograded as shown in Fig. 1. The doping in the epitaxial layer is given by

$$N_D(x) = N_0 \exp(-x/L)$$

where N_0 is the impurity atom concentration at the surface, and L is the characteristic length of the exponential decay. Application of Poisson's equation, and the depletion region approximation, yields the voltage across the depletion region width W as

$$V(W) = -\frac{q}{\epsilon} N_0 L^2 \left[\left(\frac{W}{L} + 1 \right) e^{-W/L} - 1 \right]. \quad (1)$$

The reverse breakdown voltage V_{br} for a particular combination of N_0 and L was found by determining the depletion region width $H = W(V_{\text{BR}})$ at the onset of avalanche breakdown by setting the ionization integral equation to unity

$$1 = \int_0^H A \exp\left[-\frac{b^2}{E^2(x)} \right] dx \quad (2)$$

where $A = 3.5 \times 10^5$ cm^{-1} and $b = 6.85 \times 10^5$ V cm^{-1} for GaAs as given by Sze and Gibbons [2].

The thickness of the undepleted epitaxial layer was set equal to the maximum depletion region width H, determined above in order to minimize its contribution to the device series resistance.

III. EQUIVALENT CIRCUIT

The varactor diode can be modeled as a junction capacitance in series with the resistance of the epitaxial layer and the substrate. Including the edge effects of a small anode radius, the junction capacitance is given by [3]

$$C = \frac{\epsilon_0 \epsilon_r \pi r^2}{W} \left(1 + \frac{\gamma W}{r} \right) \quad (3)$$

where r is the anode radius, ϵ_0 is the permittivity of free space, ϵ_r

0018-9480/83/0200-0235$01.00 ©1983 IEEE

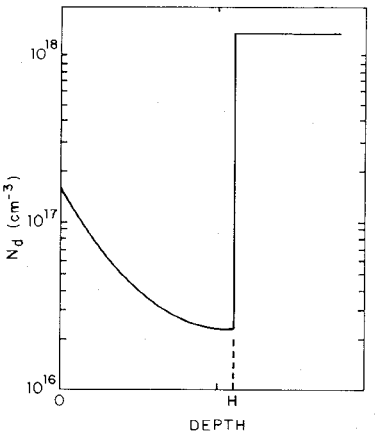

Fig. 1. Retrograded impurity profile of epitaxial layer.

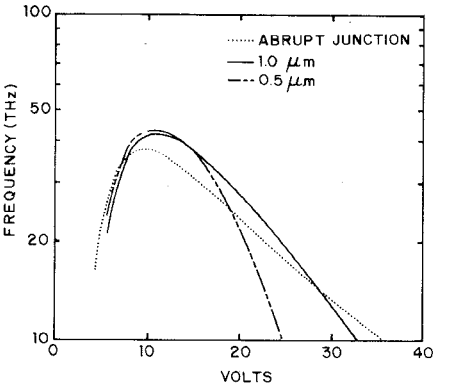

Fig. 2. Varactor dynamic cutoff frequency versus breakdown voltage for an abrupt junction and two hyperabrupt junctions having characteristic lengths (a) 0.5 μm and (b) 1 μm.

is the relative permittivity of the material, and

$$\gamma = 1.416 + \frac{1.72}{\epsilon_r}.$$

The average dynamic capacitance is defined as the time-averaged capacitance of the device when it is pumped by a sinusoidal voltage source from zero bias to breakdown.

The resistance of the undepleted epitaxial layer is given by

$$R_{\text{epi}} = \int_{W(V)}^{H} \frac{dx}{q\mu_n N(x)\pi r^2} \tag{4}$$

where q is the electronic charge, H is the epitaxial layer thickness, $W(V)$ is the depletion region depth for an applied voltage V (less than V_{br}), and μ_n is the electron mobility which is given by the expression of Hilsum [4]

$$\mu_n = \frac{10^4}{1 + \sqrt{\dfrac{N(x)}{10^{17}}}}$$

where the epitaxial layer thickness is equal to the depletion region depth at breakdown. In the case considered, this becomes

$$R_{\text{epi}} = \frac{10^{-4}}{qN_0\pi r^2} \cdot \left[e^{H/L} - e^{-W(V)/L} + 2\sqrt{\frac{N_0}{10^{17}}} \left(e^{H/2L} - e^{-W(V)/2L} \right) \right].$$

The remainder of the series resistance components, including spreading and skin effect, were determined at the operating frequency by the method of Carlson *et al.* [5].

IV. Figures of Merit

Two figures of merit indicative of device performance are dynamic cutoff frequency and normalized power. The dynamic cutoff frequency is defined by Penfield and Rafus [6] as

$$f_c = \frac{S_{\max} - S_{\min}}{2\pi R_s}$$

where $S_{\max}$ is the inverse capacitance at breakdown and $S_{\min}$ is the inverse capacitance at zero bias, and R_s is the device series resistance. The normalized power is indicative of the amount of power the device is capable of handling

$$P_{\text{norm}} = \frac{(V_{br} + V_{bi})^2}{R}.$$

V. Device Design

Using the relations developed in the preceding sections, the dynamic cutoff frequency can be plotted as a function of the reverse breakdown voltage. The epitaxial layer contribution to the total series resistance for the calculation of cutoff frequency was taken as that of the total epitaxial layer (i.e., $W(V) = 0$ in (4)) resulting in a very conservative estimate for the dynamic cutoff frequency. The results shown in Fig. 2 are based on a 5-μm diameter anode. The epitaxial layer thickness was taken to be exactly equal to the depletion region width at breakdown. The substrate was assumed to be 5 mils square and 5 mils thick. Curves for various values of L are shown.

For a desired breakdown voltage, L can be optimized for maximum cutoff frequency. Once L is selected, there is a unique value of N_0 and epi-thickness for the desired breakdown voltage as shown in Fig. 3. Breakdown voltage versus the surface impurity concentration N_0 is shown in Fig. 4. The last fabrication parameter to be determined is the anode size. This was chosen to provide a device with an average dynamic capacitance which would best match the impedance of the microwave mount.

VI. Test Results

For the first iteration of device optimization, a device with a reverse breakdown of 15 V and an average dynamic capacitance of 10 fF was chosen. This allowed the device to be tested in an existing microwave mount and to be readily compared to the performance of an optimized abrupt junction varactor designated 5M4. The hyperabrupt structure was designed to replace the abrupt junction varactor used in a 190–230-GHz frequency doubler designed and optimized by Archer *et al.* [1].

A characteristic length of 1 μm was chosen as the surface doping gradient, with the highest cutoff frequency occurring at a breakdown of 15 V. The corresponding surface impurity doping is 10^{17} cm^{-3}, and the epitaxial layer thickness is 0.6 μm. For a 5-μm diameter anode, the calculated series resistance is 6.3 Ω, and the average dynamic capacitance is 14.3 fF with a zero bias capacitance of 19.4 fF. These values are given in the left-hand column of Table I.

The retrograded Si-doped epitaxial layer was grown by MBE on a degenerated doped substrate. A 4000-Å-thick SiO_2 layer was

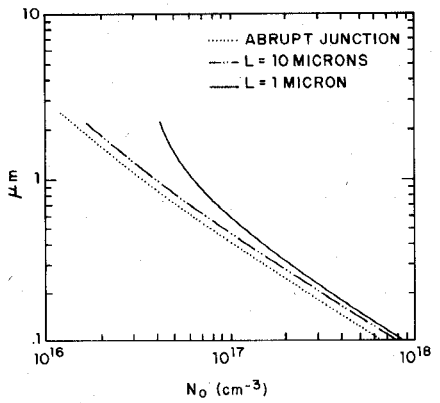

Fig. 3. Diode depletion width at breakdown versus surface doping concentration for an abrupt and two hyperabrupt Schottky-barriers having characteristic lengths (a) 1 μm and (b) 10 μm.

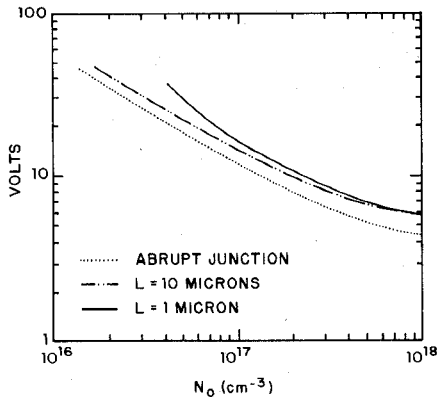

Fig. 4. Varactor reverse breakdown voltage versus surface doping concentration N_0 for a GaAs abrupt junction and hyperabrupt junctions having characteristic lengths (a) 1 μm and (b) 10 μm.

TABLE I
DESIRED, PREDICTED, AND MEASURED DC DEVICE PARAMETERS FOR HYPERABRUPT (5F1) AND ABRUPT (5M4) SCHOTTKY-BARRIER VARACTORS

		Desired device	Theoretical predictions	5F1	5M4
V_{br}	(V)	15.2	(8.1)	15.6	14.2
R_s	(Ω)	6.3	4.8	4.4	6.8
C_{jo}	(fF)	19.4	22.5	20.1	19.4
P_{norm}	(W)	41.7	----	62.6	40.0

pyrolytically deposited at 250°C with SiH_4 and O_2, through which anode openings were photolithographically defined and etched. The anodes were formed by electroplating platinum then gold. A Sn–Ni/Ni/Au ohmic contact [7] was formed on the back of the substrate. The 5-mil-thick devices were diced to 5-mil squares and contacted for dc tests.

Capacitance versus voltage data for a hyperabrupt structure, designated as 5F1, is shown in Fig. 5. The 5F1 is compared to an optimized abrupt junction device 5M4. The hyperabrupt structure exhibits the expected greater capacitance variation than the abrupt junction up to a reverse bias of 6 V. The reduced capacitance change above 6 V, in the case of the hyperabrupt device, is indicative of the depletion region sweeping onto the degenerately doped substrate. The impurity doping profile was calculated from the capacitance versus voltage data and is shown in Fig. 6. It

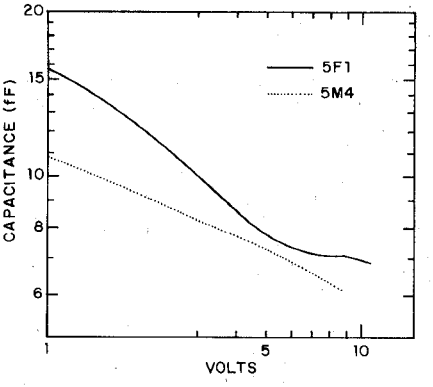

Fig. 5. Capacitance versus bias voltage for hyperabrupt (5F1) and abrupt (5M4) Schottky-barrier varactors.

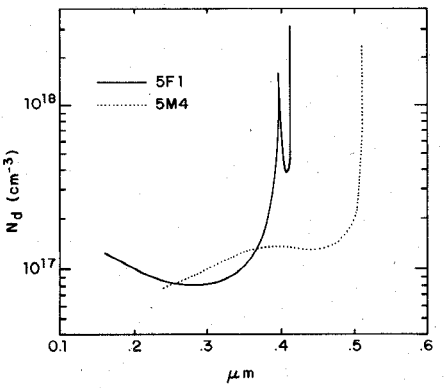

Fig. 6. Doping concentration versus depth resulting from $C(V)$ measurements for hyperabrupt (5F1) and abrupt (5M4) Schottky-barrier varactors.

should be noted that the 5F1 has a higher extrapolated surface impurity concentration (1.58×10^{17}), steeper surface gradient (characteristic length 0.31 μm), and a thinner epitaxial layer (0.4 μm), than the desired structure described above. The dc test results are presented in Table I. The column headed "Theoretical Predictions" is included as an indication of the accuracy of the modeling techniques used in this study. The values listed in the second column of Table I were calculated from the doping profile parameters listed above, which were taken from Fig. 6. The value listed for the theoretical breakdown is the voltage sustained by the epitaxial layer only, rather than the actual breakdown voltage. This indicates that the depletion region is entering the substrate well before breakdown.

The dc test results indicate that the hyperabrupt junction diode has electrical parameters superior to those of the abrupt junction. The breakdown voltage is higher, the series resistance is lower, and the capacitance modulation is greater than that of the abrupt junction.

The device was mounted, whisker contacted, in the half-height output waveguide of a crossed-guide harmonic generator similar to that described by Archer [8]. Fig. 7 shows the power conversion efficiency versus the frequency for a 5F1 and a typical 5M4 in this mount. The power conversion efficiency plotted is the ratio of the output power at the desired frequency to the input pump power of 50 mW. The conversion efficiencies of the 5F1 are as good as, or better than, those of the 5M4 over most of the 190–230-GHz range. The output-power bandwidth integral is larger for the hyperabrupt structure (234-mW GHz for the 5F1, compared to 214-W MHz for the 5M4). Also note that the peak efficiency for the 5F1 occurs at a slightly higher frequency. However, this is thought to be the result of small differences in

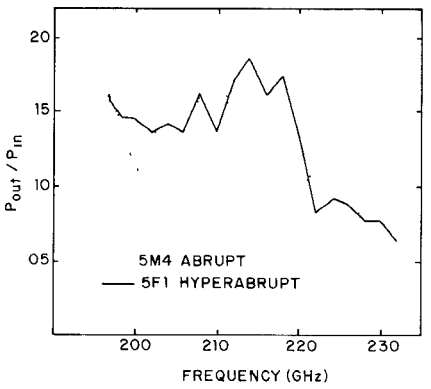

Fig. 7. Power conversion efficiency versus frequency for (a) hyperabrupt (5F1) and (b) abrupt (5M4) Schottky-barrier varactors where P_{IN} is maintained at 50 mW.

the mount geometry and average diode capacitance for the two cases evaluated.

It should be pointed out that, at this stage in harmonic generator development at 230 GHz, the losses of the mount dominate the losses of the varactor. Thus, a more efficient varactor would be expected to yield only small improvements in the performance of the frequency multiplier.

VII. Summary

The models developed to predict the electrical parameters of a hyperabrupt varactor based on its physical parameters were shown to be accurate. Reverse breakdown voltage, capacitance, and series resistance were examined as a function of the impurity doping profile, epitaxial layer thickness, and anode size.

Hyperabrupt junction devices were shown to have superior dc characteristics when compared to an equivalent abrupt junction device. The 5F1 devices exhibited higher breakdown voltages, lower series resistance, and a greater capacitance modulation than an optimized abrupt junction diode. Comparison of the behavior of 5M4 and 5F1 devices mounted in a 190–230-GHz doubler showed that the 5F1 had a larger output power bandwidth integral, and a peak efficiency at a higher frequency than the 5M4. The RF performance on both abrupt and hyperabrupt devices was limited by the characteristics of the microwave circuit.

The design, fabrication, and testing of devices in this research was aimed at competing directly with an optimized abrupt junction device in an application for which it has established its desirability. To facilitate the development of higher order frequency multipliers, with harmonic outputs of order 3 and higher, and usable output power, there is a need for devices with high breakdown voltages (25–30 V), which can handle higher pump powers, but still have a high degree of capacitance modulation. Fig. 2 indicates that the hyperabrupt structures show promise at being able to satisfy this need.

It is possible to reduce device series resistance by allowing punch-through breakdown to occur. Capacitance modulation and maximum breakdown voltage may be sacrificed to gain conversion efficiency by the reduction of power dissipation in the device.

VIII. Conclusion

The use of a hyperabrupt junction varactor diode for millimeter-wave applications was shown to be successful. Device comparison showed the hyperabrupt device to perform, in general, at least as well as the equivalent abrupt junction device. At present, the microwave circuit limits the performance of frequency multipliers in the 100–230-GHz output frequency range. However, with continued improvement in mount design, it is expected that the hyperabrupt device will yield superior conversion efficiency and power handling capabilities when compared with the abrupt junction devices in the same improved mount.

References

[1] J. W. Archer, B. B. Cregger, R. J. Mattauch, and J. D. Oliver, Jr., "Harmonic generators have high efficiency," *Microwaves*, vol 21, no 3, pp 84–87, Mar. 1982.

[2] S M Sze and G. Gibbons, "Avalanche breakdown voltages of abrupt and linearly graded p-n junctions in Ge, Si, GaAs, and GaP," *Appl. Phys Lett.*, vol. 8, no. 5, pp 111–113, Mar. 1, 1966

[3] J. A Copeland, "Diode edge effect of doping profile measurements," *IEEE Trans. Electron Devices*, vol ED-17, pp. 404–407, May 1970.

[4] C. R. Hilsum, "Simple empirical relationship between mobility and carrier concentration," *Electron Lett*, vol. 10, p. 259, 1974

[5] E. R Carlson, M V. Schneider, and T. F. McMaster, "Subharmonically pumped millimeter-wave mixers," *IEEE Trans Microwave Theory Tech*, vol MTT-26, pp. 706–715, Oct 1978.

[6] P Penfield and R P Rafuse, *Varactor Applications* Boston, MA: MIT Press, pp 86–87, 1962.

[7] A. Aydinli and R. J Mattauch, "Au/Ni/Sn–Ni/n–GaAs interface: Ohmic contact formation," *J Electrochem. Soc*, vol. 128, no. 12, pp. 2635–2638, Dec. 1981.

[8] J. W Archer, "Millimeter wavelength frequency multipliers," *IEEE Trans. Microwave Theory Tech.*, vol. MTT-29, pp 552–557, June 1981

A Limiter for High-Power Millimeter-Wave Systems

ALBERT L. ARMSTRONG, SENIOR MEMBER, IEEE, AND YOGI ANAND, MEMBER, IEEE

***Abstract*—A high-power limiter for use in millimeter-wave systems has been designed and demonstrated. The RF control is provided by an array of p-i-n diodes fabricated into the surface of a high-resistivity silicon window. Orientation-dependent etching of the silicon is used to build diodes with parallel injection surfaces. The window is mounted into the waveguide using a metal membrane which simplifies construction and lowers cost.**

I. Introduction

In high-power communication and radar systems, power limiter components are used in front of the mixer diode for RF burnout protection. Typically, a limiter may need to provide 20–50-dB attenuation for high-level signals while minimum possible loss is desired for low-level signals. In addition, if the limiter is of the

Manuscript received July 16, 1982; revised September 10, 1982. This work was supported in part by USA-ERADCOM under contract DAAK20-81-C-0395, J Armata, contract Monitor.

A. Armstrong is a Consultant to M/A-Com Millimeter Products, Inc and is President of Capitol Technology Corporation, Latham, N.Y. 12110.

Yogi Anand is with M/A-Com Millimeter Products, Inc, Burlington, MA 01803.

0018-9480/83/0200-0238$01.00 ©1983 IEEE